Algorithms for Molecular Biology

SOFTWARE Open Access

Pangenomic genotyping with the marker array

Taher Mun[1], Naga Sai Kavya Vaddadi[1] and Ben Langmead[1*]

Abstract
We present a new method and software tool called `rowbowt` that applies a pangenome index to the problem of inferring genotypes from short-read sequencing data. The method uses a novel indexing structure called the marker array. Using the marker array, we can genotype variants with respect from large panels like the 1000 Genomes Project while reducing the reference bias that results when aligning to a single linear reference. `rowbowt` can infer accurate genotypes in less time and memory compared to existing graph-based methods. The method is implemented in the open source software tool `rowbowt` available at https://github.com/alshai/rowbowt.

Keywords Sequence alignment, Indexing, Genotyping

Introduction

Given DNA sequencing reads from a donor individual, genotyping is the task of determining which alleles the individual has at polymorphic sites. Genotyping from sequencing data, sometimes using low-coverage sequencing data together with genotype imputation, is a common task in human genetics [1] and agriculture [2]. In contrast to variant calling, genotyping is performed with respect to a catalog of known polymorphic sites. For instance, genotyping of a human can be performed with respect to the 1000 Genomes Project call set, which catalogs positions, alleles and allele frequencies for tens of millions of sites [3].

Many existing genotypers start by aligning reads to a single linear reference genome, e.g. the human GRCh38 reference [4]. Because this reference is simply one example of an individual's genome, genotyping is subject to reference bias, the tendency to make mistakes in places where the donor differs genetically from the reference. This was shown in studies of archaic hominids [5], HLA genotypes [6] and structural variants [7]. A similar bias exists for methods that extract polymorphic sites along with genomic context, and search for these sequences in the reads [8, 9]. In particular, the bias remains if the flanking sequences are extracted from the reference and so contain only reference alleles.

Reference bias can be reduced by using a *pangenome* reference instead of a single linear reference. A pangenome can take various forms; it can be (a) a generating graph for combinations of alleles, (b) a small collection of linear references indexed separately, or (c) a larger collection of linear reference indexed together in a compressed way. Pangenome graphs (option a) and small collections of linear references (option b) have been studied in recent literature [10–14].

Two existing methods that use pangenome graphs are `BayesTyper` [15] and `PanGenie` [16]. `BayesTyper` works by matching k-mers extracted from the input reads to k-mers stored in a de Bruijn graph representing known polymorphisms and their surrounding contexts. After tallying this evidence, `BayesTyper` calls genotypes based on a generative model. `PanGenie` uses a graph built from haplotypes, collapsed so that variants become bubbles. `PanGenie` then scans the reads and tallies k-mers that appear in the graph. It then makes genotype

*Correspondence:
Ben Langmead
langmea@cs.jhu.edu
[1] Department of Computer Science, Johns Hopkins University, Baltimore, MD, USA

calls based on the tallies of how often read k-mers match to k-mers along the alternate paths that make up the distinct REF and ALT alleles.

Variant graphs like the ones used by `BayesTyper` and `PanGenie` are effective for genotyping, but have drawbacks when the goal is to reduce reference bias. First, haplotype information might be removed when adding variants to the graph, or might be included in the graph but not considered during the read mapping process. This can cause graph-based tools to consider many extraneous haplotype paths through the graph during genotyping, increasing running time. Second, variant graphs can grow exponentially—in terms of the number of paths through the graph—as variants are added, leading to a rapid increase in resource usage and likelihood of ambiguous alignments.

We sought a way to reduce reference bias by indexing and querying many linear references at once while keeping index size and query time low. Such an approach can take full advantage of linkage disequilibrium information in the panel, allowing no recombination events except those occurring in the panel. This avoids mapping ambiguity from spurious recombination events between polymorphic sites [10].

We propose a new structure called the *marker array* that replaces the suffix-array-sample component of the r-index with a structure tailored to the problem of collecting genotype evidence. Here we describe the marker array structure in detail. We compare its space usage and query time to those of the standard r-index and explore how accurately both structures are able to capture markers from a sequencing dataset. Finally, we benchmark it using real whole-genome human sequencing data and compare it to the `BayesTyper` and `PanGenie` genotyping tools in terms of both genotyping accuracy and computational efficiency. We do this for variants genomewide and for variants in genes that are medically relevant.

Background

r-index

The r-index [17] is a compressed repeat-aware text index that scales with the non-redundant content of a sequence collection. It uses $O(r)$ space where r is the number of same-character *runs* in the Burrows-Wheeler Transform (BWT) of the input text. Past work shows that the r-index can efficiently index collections of long-read-derived human genome assemblies [18] as well as large collections of bacterial genomes [19].

While the main contribution of the r-index was its strategy for storing and using a sample of the suffix array [17], even this sample is large in practice. We propose a new *marker array* structure that replaces the suffix array while retaining its ability to deduce when a read-to-pangenome match provides evidence for a particular allele at a polymorphic site. The design of the marker array flows from three observations. First, we can save space by storing auxiliary information about polymorphic sites ("markers") only at the sites themselves. There are often far fewer sites harboring polymorphism than there are BWT runs. Second, pangenome suffixes starting with the same allele tend to group together in the suffix array, which can be exploited to compress the marker array structure. Third, while a suffix array entry is an offset into the pangenome requiring $O(\log n)$ bits, a marker need only distinguish markers and alleles, and so requires just $O(\log M)$ bits where M is the number of polymorphic sites.

Methods

Preliminaries

Consider a string S of length n from ordered alphabet Σ, with operator $\prec$ denoting lexicographical order. Assume S's last character is lexicographically less than the others. Let F be an array of S's characters sorted lexicographically by the suffixes starting at those characters, and let L be an array of S's characters sorted lexicographically by the suffixes starting immediately after them. The list L is the Burrows-Wheeler Transform [20] of S, abbreviated BWT.

The BWT can function as an *index* of S [21]. Given a pattern P of length $m < n$, we seek the number and location of all occurrences of P in S. If we know the range $\mathsf{BWT}(S)[i..j]$ occupied by characters immediately preceding occurrences of a pattern Q in S, we can compute the range $\mathsf{BWT}(S)[i'..j']$ containing characters immediately preceding occurrences of cQ in S, for any character $c \in \Sigma$, since

$$i' = |\{h : S[h] \prec c\}| + |\{h : \mathrm{BWT}(S)[h] = c, h < i\}|. \tag{1}$$

$$j' = |\{h : S[h] \prec c\}| + |\{h : \mathrm{BWT}(S)[h] = c, h \leq j\}| - 1. \tag{2}$$

The FM Index is a collection of data structures for executing such queries efficiently. It consists of an array C storing $|\{h : S[h] \prec c\}|$ for each character c, plus a rank data structure for $\mathsf{BWT}(S)$, e.g. a wavelet tree, that can quickly tally the occurrences of a character c up to a position of BWT. To locate the offsets of occurrences of P in S, the FM-index can additionally include some form of S's suffix array. The suffix array SA is an array parallel to F containing the offsets of the characters in F. To save space, the FM-index typically keeps only a sample of SA, e.g. a subset spaced regularly across SA or across S.

Let $T = \{T_0, T_1, \ldots, T_n\}$ be a collection of n similar texts where T_0 is the *reference sequence*, and $T_1, \ldots, T_n$

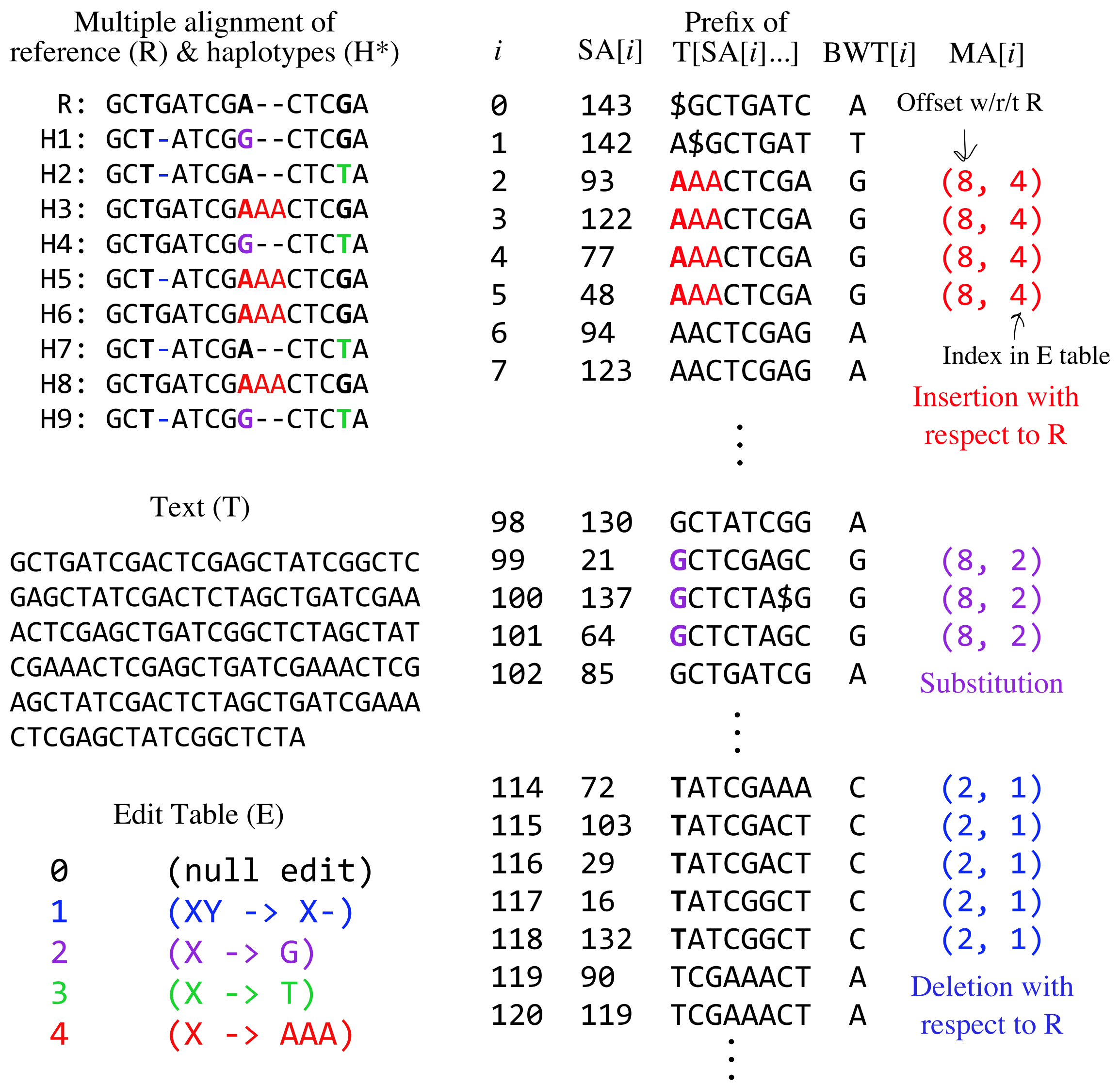

Multiple alignment of reference (R) & haplotypes (H*)

```
 R: GCTGATCGA--CTCGA
H1: GCT-ATCGG--CTCGA
H2: GCT-ATCGA--CTCTA
H3: GCTGATCGAAACTCGA
H4: GCTGATCGG--CTCTA
H5: GCT-ATCGAAACTCGA
H6: GCTGATCGAAACTCGA
H7: GCT-ATCGA--CTCTA
H8: GCTGATCGAAACTCGA
H9: GCT-ATCGG--CTCTA
```

Text (T)

```
GCTGATCGACTCGAGCTATCGGCTC
GAGCTATCGACTCTAGCTGATCGAA
ACTCGAGCTGATCGGCTCTAGCTAT
CGAAACTCGAGCTGATCGAAACTCG
AGCTATCGACTCTAGCTGATCGAAA
CTCGAGCTATCGGCTCTA
```

Edit Table (E)

0	(null edit)
1	(XY -> X-)
2	(X -> G)
3	(X -> T)
4	(X -> AAA)

i	SA[i]	Prefix of T[SA[i]...]	BWT[i]	MA[i]
0	143	$GCTGATC	A	
1	142	A$GCTGAT	T	
2	93	AAACTCGA	G	(8, 4)
3	122	AAACTCGA	G	(8, 4)
4	77	AAACTCGA	G	(8, 4)
5	48	AAACTCGA	G	(8, 4)
6	94	AACTCGAG	A	
7	123	AACTCGAG	A	
		⋮		
98	130	GCTATCGG	A	
99	21	GCTCGAGC	G	(8, 2)
100	137	GCTCTA$G	G	(8, 2)
101	64	GCTCTAGC	G	(8, 2)
102	85	GCTGATCG	A	
		⋮		
114	72	TATCGAAA	C	(2, 1)
115	103	TATCGACT	C	(2, 1)
116	29	TATCGACT	C	(2, 1)
117	16	TATCGGCT	C	(2, 1)
118	132	TATCGGCT	C	(2, 1)
119	90	TCGAAACT	A	
120	119	TCGAAACT	A	
		⋮		

Fig. 1 Top left: A multiple alignment for a collection of alternate haplotypes (H1–H9), and a reference sequence (R). Marked bases are in bold and alternate alleles are colored. Middle left: The text *T*, formed by concatenating rows of the multiple alignment (eliding gaps). Bottom left: The edit table *E*, with alternate-allele coloring. Right: A partial illustration of the marker array in relation to SA, the relevant suffixes themselves (truncated to fit), and the BWT. Colors and bolding highlight where marked bases and alternate alleles end up in the suffixes

are *alternative sequences*. In the scenarios studied here, a T_i represents a human haplotype sequence, with all chromosomes concatenated, and T_0 represents the GRCh38 primary assembly of the human genome. Each T_i with $i > 0$ is an alternate haplotype taken either from the 1000 Genomes project call set [3] or from the HGSVC project [22, 23], each with chromosomes concatenated in the same order as T_0's. We use the terms "haplotype" and "genome" interchangeably here.

We assume that all the T_i's are interrelated through a multiple alignment, e.g. as provided in a Variant Call Format (VCF) file. The multiple alignment is a matrix with genomes in rows and columns representing genomic offsets. The elements are either bases or gaps. We call a column consisting of identical bases and lacking any gaps a *uniform* column. Any other column is a *polymorphic* column. Figure 1 illustrates a multiply-aligned collection of haplotypes and the concatenated text T.

Marker array

Let the "marker array" M be an array parallel to the concatenated sequence T marking positions that fall in a polymorphic column in the multiple alignment. Each element of M is a tuple recording the offset i with respect to T_0 where the polymorphism begins, as well as the edit operation describing how the sequence differs from the reference at this locus. Distinct edit operations are given distinct integer identifiers, which are decoded using a separate table E. Identifier 0 is the null operation, denoting that the reference allele appears without edits. For example, say $E = \{1 : X \to C\}$, where $X \to C$ denotes a substitution that replaces the reference base with C. Then a marker array record $m = (500, 0)$ marks a locus with no edit with respect to reference position $T_0[500]$. A record $m' = (500, 1)$ denotes that a substitution changes that base at $T_0[500]$ to a C. An example is shown in Fig. 1 (bottom left).

Consecutive substitutions are collapsed into a single edit in the E table. Insertions and deletions ("indels" for short) are treated somewhat differently; the offset carrying the "mark" is the one just preceding the indel (just to its left) in the multiple alignment. Importantly, the mark covers exactly one position in the genome, even if the insertion/deletion spans many bases. The marked position must come to the left of the indel to ensure that suffixes starting at the marked position include the allele itself. In the multiple alignment in Fig. 1 (top left), for example, a deletion with respect to R occurs in the fourth-from-left column, but the marked position is in the third-from-left column.

The marker array MA is a permutation of M such that marks appear in suffix-rank order:

Definition 1 The *marker array* MA is the mapping such that $\mathsf{MA}[i] = \mathsf{M}[\mathsf{SA}[i]]$.

Thanks to suffix-rank order, identical $\mathsf{M}[i]$'s are often grouped into runs in MA, as seen in Fig. 1 (right).

A *marker query* for pattern string q returns all $m \in \mathsf{M}$ overlapped by an occurrence of q in T. We can begin to answer this query using backward search (Eq. 1) with $P = q$, giving the maximal SA range $[i..j]$ such that q is a prefix of the suffixes in the range. Having computed $[i..j]$, we know that $\{\mathsf{MA}[i], ..., \mathsf{MA}[j]\}$ contain markers overlapped by q's leftmost character. To recover the markers overlapped by the rest of q's characters, two approaches can be considered, detailed in the following subsections. The *FL* approach recovers the overlapped markers in a straightforward way but uses $O(|q| \cdot \mathsf{occ})$ time, where occ is the number of times q occurs in T. The heuristic backward-search approach requires only $O(|q|)$ time but is not fully sensitive, i.e. it can miss some overlaps.

FL approach

Say $[i..j]$ is the maximal SA range such that all rows have q as a prefix. We can perform a sequence of FL steps, starting from each row $x \in [i..j]$. An FL step is the inverse of an LF step. That is, if we write an LF mapping step in terms of a rank query

$$i' = |\{h : S[h] \prec c\}| + \mathsf{BWT}.\mathrm{rank}_{\mathsf{BWT}[i]}(i), \tag{3}$$

where $S.\mathrm{rank}_c(i)$ denotes the number of occurrences of c in S up to but not including offset i, then an FL step inverts this using a select query

$$i = \mathsf{BWT}.\mathrm{select}_{F[i']}(i' - |\{h : S[h] \prec F[i']\}|), \tag{4}$$

where $S.\mathrm{select}_c(i)$ returns the offset of the $i + 1^{\text{th}}$ occurrence of c in S, i.e. the c of rank i. Whereas LF takes a leftward step with respect to T, FL takes a rightward step.

By starting in each row $x \in [i..j]$ and performing a sequence of $|q| - 1$ FL steps for each, we can visit each offset of T overlapped by an occurrence of q. Checking $\mathsf{MA}[k]$ at each step, where k is the current row, tells us which marker is overlapped, if any. This is slow in practice, both because it requires $O(|q|(j - i + 1))$ FL steps in total, and because each step requires a select query, which is more costly in practice than a rank query.

Heuristic backward-search approach with smearing

Say we perform a backward search starting with the rightmost character of q. At each step we are considering a range $[i..j]$ of SA having a suffix of q as a prefix. Using i and j, we can query $\mathsf{MA}[i..j]$. However, this tells us instances where a *suffix* of q overlaps a marker, whereas our goal is to find where the *whole* query q overlaps a marker. If we report overlaps involving trivially short suffixes of q, many would be false positives. We propose to allow but reduce the number of such false positives by augmenting MA:

Definition 2 The *augmented marker array* MA^w is a multimap such that $\mathsf{MA}^w[i] = [\mathsf{M}[\mathsf{SA}[i]], \mathsf{M}[\mathsf{SA}[i] + 1], ..., \mathsf{M}[\mathsf{SA}[i] + w]]$

That is, $\mathsf{MA}^w[i]$ is a (possibly empty) list containing markers overlapping any of the positions $T[i..i + w]$. We call this a "smeared" marker array, since the marks are extended (smeared) to the left by w additional positions. Note that a length-w extension can overlap one or more other marked variants to the left. For this reason, MA^w must be a multimap, i.e. it might associate up to w markers with a given position.

Using MA^w, we adjust the backward-search strategy so that instead of querying MA at each step, we query MA^w every w steps. If w is large enough—e.g. longer than the length at which we see random-chance matches—we can avoid many false positives. More space is required to represent MA^w compared to MA since it is less sparse. However, we expect MA^w to remain run-length compressible for the same reason that MA is.

Genotyping a read

Given a sequencing read, we would like to extract as much genotype information as possible while minimizing computational cost and false-positive genotype evidence. Here we give a heuristic algorithm (Algorithm 1) that handles entire sequencing reads, querying MA^w during the backward-search process as proposed in the previous section. The algorithm proceeds right to left through the read, growing the match by one character if possible. When we can no longer grow the match (i.e. the range $[i..j]$ becomes empty), we reset the range to the all-inclusive range $[0..|T|-1]$ and restart the matching process at the next character. We use the term "extension" to refer to a consecutive sequence of steps that successfully extend a match. Note that this is a heuristic algorithm that does not exhaustively find all half-MEMs between the read and the index, as the MONI algorithm does [24].

Algorithm 1 Simplified version of `rowbowt` algorithm for matching query string q and compiling genotype evidence. C is an array such that $C[c]$ equals $|\{h : T[h] \prec c\}|$, where T is the original text. N_h is the number of haplotypes in the index. Pseudocode for TallyEvidence and FinalizeEvidence are not given, but the heuristics they use to further filter genotype evidence is described in the text.

```
1: procedure SIMPLEGENOTYPE($q$, $w$, $\mathsf{MA}^w$, BWT, $C$, $N_h$)
2:     $i = 0,\ j = |BWT|$
3:     $\ell = 0,\ k = 0$                                        ▷ start new extension
4:     $o = |q| - 1$
5:     while $o \geq 0$ do
6:         $c = q[o]$
7:         $i = C[c] + \mathsf{BWT.rank}_c(i)$          ▷ backward search, like equations 1 and 2
8:         $j = C[c] + \mathsf{BWT.rank}_c(j)$
9:         if $i = j$ then                                   ▷ no matching substrings
10:            FinalizeEvidence($\ell$)    ▷ ignore tallied evidence if $\ell$ is small or evidence conflicts
11:            $i = 0,\ j = |BWT|,\ k = 0,\ \ell = 0$                 ▷ start new extension
12:        else
13:            $k = k + 1,\quad \ell = \ell + 1$
14:            if $k = w$ then
15:                if $(j - i + 1) \leq N_h$ then
16:                    for $x \in [\,i\,..\,j\,)$ do
17:                        for $site \in \mathsf{MA}^w[x]$ do
18:                            TallyEvidence($site$)      ▷ increment evidence for allele at site
19:                        end for
20:                    end for
21:                end if
22:                $k = 0$                                   ▷ check every $w$ steps
23:            end if
24:        end if
25:        $o = o - 1$
26:    end while
27:    FinalizeEvidence($\ell$)        ▷ ignore tallied evidence if $\ell$ is small or evidence conflicts
28: end procedure
```

As discussed above, the algorithm only checks the marker array every w steps (line 14). As an additional filter, the algorithm only performs a marker-array query when the current suffix-array range size is no larger than the number of haplotypes in the index (N_h). A range exceeding that size indicates that we are seeing more than one distinct match in at least one haplotype, meaning that the evidence is ambiguous.

The algorithm tallies evidence as it goes (line 18), but might later choose to ignore that evidence if certain conditions are not satisfied (lines 10 and 27). For example, if the evidence has a conflict—i.e. one match indicates a reference allele at a site but another match found during the same extension finds an alternate allele at that site—then all the evidence is discarded for that extension. Similarly, evidence from an extension is discarded if the tallied sites span multiple chromosomes. Finally, evidence from extensions failing to match at least 80 bp of the read (adjustable with `--min-seed-length` option) is discarded.

We employ other heuristics to minimize mapping time not shown in Algorithm 1. For instance, we avoid wasted effort spent querying the wrong read strand. Specifically: `rowbowt` randomly selects an initial strand of the read to investigate: forward or reverse complement. If an extension from this strand meets the minimum seed-length threshold (80 by default), then the other strand is not considered and analysis of the read is complete. Otherwise, `rowbowt` then goes on to examine the opposite strand of the read.

Sparse marker encoding

We encode the sparse arrays M, MA and MA^w in the following way. Say that array A consists of empty and non-empty elements. We consider A's non-empty elements as falling into one of x maximal runs of identical (and non-empty) elements. Our sparse encoding for A consists of three structures. S is a length-$|A|$ bit vector with 1s at the positions where a run of identical entries in A begins, and 0s elsewhere. E is a similar bit vector marking the last position of each of the x runs. (This variable E is distinct from the E table defined above in "Marker Array.") To find whether an element $A[i]$ is non-empty, we can ask whether we are between two such marks; that is, $A[i]$ is non-empty if and only if $S.\text{rank}_1(i+1) > E.\text{rank}_1(i)$.

X is a length-x array containing the element that is repeated in each of A's non-empty runs, in the order they appear in A. If $A[i]$ is not empty, the element appearing there is given by $X[E.\text{rank}_1(i)]$.

When encoding M or MA, the elements of X are simply tuples. A complication exists for MA^w, since elements are lists of up to w tuples. In this case, we keep an additional bit-vector B of size $|X|$ where 1s denote left-hand boundaries in X that correspond to runs in A. E and B can be used together to access an element in A (Algorithm 2).

Algorithm 2 Access the contents of $A[i]$ in the case where entries of A can be lists

```
procedure SparseAccess($S$, $E$, $X$, $B$, $i$)
    if $S.\text{rank}_1(i+1) = E.\text{rank}_1(i)$ then
        return $\emptyset$
    end if
    $e = E.\text{rank}_1(i)$
    $j = B.\text{select}_1(e)$
    $k = B.\text{select}_1(e+1)$
    return $\{X[j], ..., X[k-1]\}$
end procedure
```

Extracting markers from VCF

A Variant Calling Format (VCF) [25] file is used to encode a collection of haplotypes with the variants arranged in order according to a reference genome. In the case of human and other diploid genomes, haplotypes are grouped as pairs. We refer to such a collection of haplotypes as a "panel" and a single haplotype as a "panelist." An VCF entry encodes a variant as a tuple consisting of a chromosome, offset, the allele found in the reference, the alternate allele found in one or more panelists, and a sequence of flags indicating whether each panelist has the reference or alternate version. We start from a VCF file to determine how to populate the marker arrays M, MA and/or MA^w, as well as the edit array E.

A single element of M is a tuple (r, e), where r is an offset in T_0 and e is the edit operation describing how the sequence differs from the reference. As a practical matter, we represent these tuples in a different way that more closely resembles the corresponding VCF records. Specifically, a marker is encoded in a 64-bit word divided into three fields. First, a 12 bit field identifies the chromosome containing the marker. The chromosome ordering is given at the beginning of the VCF file in the "header" section. For example, if "chr1" is the first chromosome in the header, then this chromosome is encoded as `0x000` (using hexadecimal), and if "chr2" is the second chromosome, it is encoded as `0x001`. Second is a 54 bit field encoding the marker's offset within the chromosome. Third is a 4-bit field storing which version of the variant is present, with 0 indicating the reference allele, 1 indicating the 1st alternate allele, 2 the second alternate allele, etc. This 64-bit representation allows for compact storage of markers and easier random access to the marker array.

Diploid genotyping

In a diploid genome, it is possible for both alleles to occur, i.e. for the genotype to be heterozygous. We use an existing approach [26] to compute genotype likelihoods considering all possible diploid genotypes: homozygous reference (2 reference alleles), homozygous alternate (2 alternate alleles), or heterozygous (1 reference, 1 alternate). Let $g \in \{0, 1, 2\}$ denote the number of reference-allele copies at the marked site; e.g. $g = 1$ corresponds to a heterozygous site and $g = 2$ to a homozygous reference site. Let l be the number of times the reference allele was observed in the reads overlapping a particular marked site and let k be the count of all alleles (reference or alternate) observed. Let ϵ be the sequencing error rate. We calculate the genotype likelihood as follows, adopting equation 2 of [26] while setting the ploidy to 2 and adopting a global rather than a per-base error rate:

$$L(g) = \frac{1}{2}^k [(2-g)\epsilon + g(1-\epsilon)]^k [(2-g)(1-\epsilon) + g\epsilon]^{k-l}.$$

To choose the most likely genotype g_{max}, we compute:

$$g_{max} = \text{argmax}_{g \in \{0,1,2\}} L(g).$$

By default, `rowbowt` uses $\epsilon = 0.01$.

Implementation details

The code for constructing the marker array is implemented in the `pfbwt-f` spoftware package, with repository at https://github.com/alshai/pfbwt-f. This repository also contains an efficient implementation of the prefix-free-parse BWT construction algorithm [18]. This software is written in C++17, uses the open-source MIT license, and builds on the Succinct Data Structure Library (SDSL) v3.0 [27].

For querying the marker array, we use the `rowbowt` implementation at https://github.com/alshai/rowbowt. This repository contains the open source C++17 implementation of `rowbowt`, distributed under the MIT license. It is also a library, containing algorithms for building and querying indexes containing various structures discussed here, including the run-sampled suffix array, marker array, and others.

Results

We evaluated the efficiency and accuracy of our marker-array method for compiling genotype evidence. We first generated multiple series of `rowbowt` indexes covering various settings for three parameters: the window size w for the smeared marker array MA^w, the number of haplotypes indexed, and the minimum allele frequency for marked alleles. The `rowbowt` index consisted of three components: the run-length encoded BWT, the run-sampled suffix array, and the marker array. While we built the sampled suffix array for these experiments, the standard marker-array-based method in `rowbowt` does not require this array.

We generated indexes for collections of 200, 400, 800, or 1000 human chromosome-21 haplotypes from the 1000 Genomes Phase 3 reference panel [3] based on the *GRCh*37 reference. We generated two sets of indexes: one where the marker array marks all polymorphic sites regardless of frequency (denoted "$AF > 0$"), and another where the marker array marks only those sites where the less common allele occurs in greater than 1% of haplotypes, i.e. has allele frequency over 1% (denoted "$AF > 0.01$"). In all cases, the marker array window size w was set to 19. Each haplotype collection was drawn from a random subset of 500 individuals from the 1000 Genomes Phase 3 panel. The $AF > 0$ panel of 500 haplotypes contained 1, 097, 388 polymorphic sites. The $AF > 0.01$ panel of the same haplotypes contained 193, 438 polymorphic sites with allele frequency over 1%. We also included the GRCh37 reference sequence, consisting of all reference alleles, in each collection, corresponding to the reference sequence called T_0 above.

We generated a series of indexes with window size $w \in \{13, 15, 17, 19, 21, 23, 25\}$. We generated two such series: one with no minimum allele frequency ($AF > 0$) and another with a 1% minimum frequency ($AF > 0.01$). Each index was over the same set of 100 haplotypes.

Index size

We measured the size of the three main components of the `rowbowt` index: the augmented marker array,

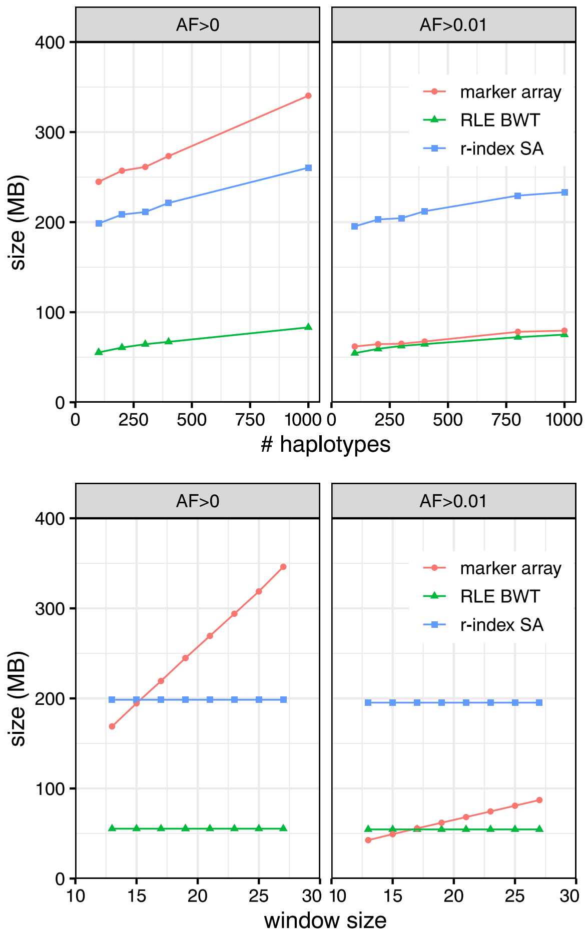

Fig. 2 Left: Size of `rowbowt` data structures as a function of the number of haplotypes indexed, and with $w = 19$. "Marker array" refers to the augmented marker array, MA^w. Right: Size of `rowbowt` data structures as a function of the "smearing" window size w, with number of haplotypes fixed at 100. Separate results are shown for when there is no minimum allowed allele frequency ($AF > 0$) and when the minimum frequency is 1% ($AF > 0.01$)

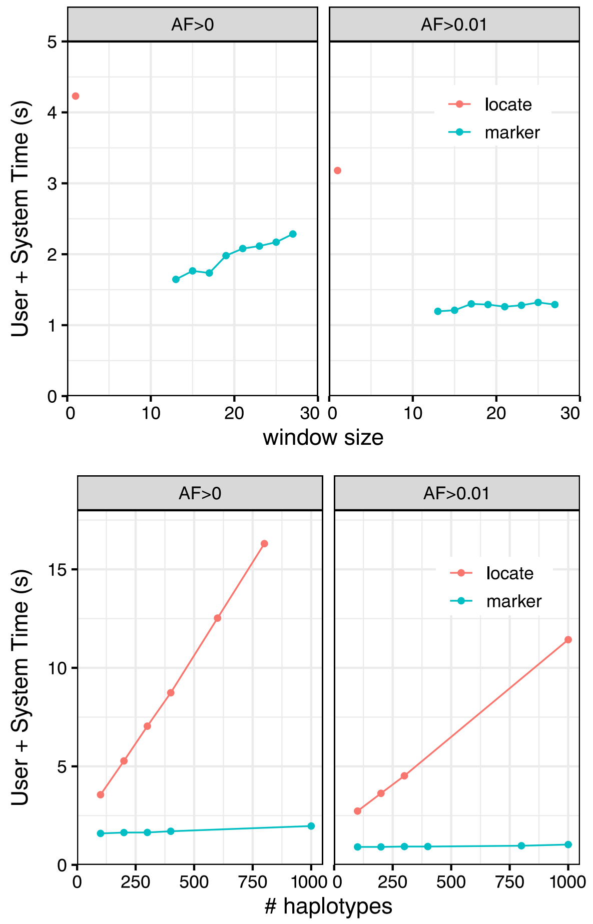

Fig. 3 Mean time over 10 trials of aligning 10,000 simulated reads from HG01498 against the augmented marker array (marker) and the r-index suffix array (locate). Experiments are repeated for marker collections including all alleles ($AF > 0$) and for alleles having frequency at least 1% ($AF > 0.01$). Left: The experiment is repeated for various window sizes w, and for 100 haplotypes. Right: The experiment is repeated for different numbers of indexed haplotypes, with $w = 19$

the run-length encoded BWT (RLE BWT) [28] and the run-sampled suffix array ("r-index SA") [17]. Figure 2 plots this measurement for collections of 200, 400, 800 and 1000 haplotypes for both $AF > 0$ and $AF > 0.01$. All grow linearly with the number haplotypes grows, as expected. For $AF > 0$, the augmented marker array is consistently larger than the run-sampled suffix array ("r-index SA"). For $AF > 0.01$, the augmented marker array is much smaller, approaching the size of the RLE BWT. The $AF > 0$ array is larger because it contains polymorphic sites with infrequent alleles; about 85% of the marked sites in the $AF > 0$ array have allele frequency under 1%. Further, rare alleles are less likely to form long runs in the augmented marker array, negatively affecting run-length compression.

In the right portion of Fig. 2, the RLE BWT and r-index SA have constant size because the w parameter does not affect those data structures. In the left portion of Fig. 2, showing size as a function of number of haplotypes, the augmented marker array is almost always larger than the r-index SA for $AF > 0$ as opposed to $AF > 0.01$, except at $w = 13$. The slope of the array size is smaller for $AF > 0.01$ than for $AF > 0$.

Overall, both the value of w and the number of haplotypes in the index cause the augmented marker array to increase in size, but the inclusion of rare alleles (< 1% allele frequency) has the largest effect on its size.

Query time

We next measured query time for the augmented marker array strategy versus the locate-query strategy which uses the run-sampled suffix array. 150 bp simulated reads of 25x coverage were generated for one haplotype of HG01498, an individual that is part of the 1000-Genomes panel, but which we excluded from all our indexes. We simulated reads using Mason 2 `mason_simulator` [29] with default options.

In the case of the marker-array strategy, we measured the time required to analyze the reads using the algorithm described above in "Genotyping a read." In the case of the locate-query strategy, the MA^w query was replaced with a two-step process that first performed a locate query with respect to the run-sampled suffix array, then performed a lookup in the M array. To enable this mode, we further augmented the *r*-index with a representation of M using the sparse encoding described above. To emphasize: the `rowbowt` strategy does not require the run-sampled suffix array or the M array; the MA^w effectively replaces them both.

We repeatedly sampled 10,000 simulated reads and recorded the mean query time over 10 trials. As seen in Fig. 3 the augmented marker-array method (labeled "marker") was consistently faster than locate method. This was true for all allele frequencies and window sizes tested. We found that the effect of w and allele-frequency cutoff was more pronounced with the larger reference panel $AF > 0$. For the smaller panel ($AF > 0.01$), query time was mostly invariant to both window size and allele frequency.

Genotyping accuracy

We next measured the accuracy of the genotype information gathered using the augmented marker array. We simulated sequencing reads from one haplotype of HG01498 to an average depth of 25-fold coverage. Individual HG01498 was excluded from the indexes. As our "truth" set for evaluation, we use the variant calls in the 1000 Genomes project callset for the same haplotype we simulated from. For simplicity, this experiment treats the genome as haploid. Experiments in the next section will account for the diploid nature of human genomes.

A single marked site can have conflicting evidence, due, for instance, to mismapped reads or sequencing errors. For this evaluation, we make calls simply by finding the frequently observed allele at the site. We ignore any instances of alleles other than the ones noted in the VCF file as the reference and alternate alleles. If the reference and alternate alleles have equal evidence, the reference allele is called.

We calculate precision and recall according to the following formulas. Here, the positive class consists of marked sites that truly have the alternate allele, while the negative class consists of marked sites that truly have the reference allele. We measure:

$$\text{Precision} = \frac{\text{TP}s}{\text{TP}s + \text{FP}s} \qquad \text{Recall} = \frac{\text{TP}s}{\text{TP}s + \text{FN}s},$$

where TP stands for True Positive, FN stands for False Negative, etc.

Figure 4 shows precision and recall with respect to the number of haplotypes in the index and the minimum allele frequency of the haplotype collection. We observed that the $AF > 0.01$ indexes generally had better precision compared to the $AF > 0$ indexes, though at the expense of recall. Precision and recall generally improve with the addition of more haplotypes to the index. The augmented marker array has similar recall to the locate procedure across all haplotype sizes at the loss of precision. When

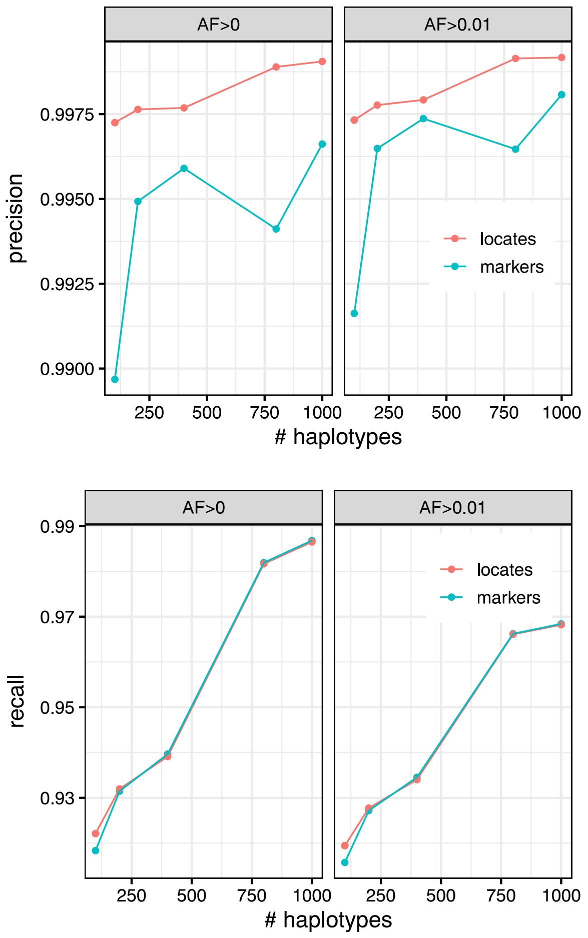

Fig. 4 Precision (left) and recall (right) of the calls made when querying 25x simulated reads from HG01498 against the augmented marker array (marker) and the *r*-index (locate). Stratified by minimum allowed allele frequency (AF) in the index

rare variants are removed from the index ($AF > 0.01$), the gap in precision between the marker array and the locate procedure lessens. This mild (less than 0.1%) loss of precision is expected since algorithm described above in "Genotyping reads" is still prone to some false positives in the earlier part of the extension process.

Diploid genotyping assessment

To assess diploid genotyping accuracy, we used data from the Human Genome Structural Variation Consortium (HGSVC) [22, 23]. The HGSVC called both simple and complex genetic variants across a panel of 64 human genomes. Calls were made with respect to the GRCh38 primary assembly [4]. For input reads, we subsampled reads from a 30-fold average coverage PCR-free read set provided by the 1000 Genomes Project [3] (accession SRR622457). To create more challenging scenarios for the genotypers, we randomly subsampled the read sets to make smaller datasets of 0.01, 0.05, 0.1, 0.5, 1, 2 and 5-fold average coverage.

We assessed four genotyping methods. The first (`bowtie2+bcftools`) used Bowtie 2 [30] v2.4.2 to align reads to a standard linear reference genome, then used BCFtools v1.13 to call variants (i.e. genotypes) at the marked sites [26]. The second method used the graph-based genotyper `BayesTyper` v1.5. The third was `PanGenie` [16], a pangenome-based genotyper for short reads. `PanGenie` calls genotypes for variants that are represented in its index as bubbles in a pangenome. `PanGenie` represents known haplotypes as paths through the graph, accounting for these paths during the genotyping process. `PanGenie` takes directed acyclic pangenome graph as input, represented as a VCF file containing phased genotypes for many samples. `PanGenie` further requires that the VCF have non-overlapping variants. We generated a compliant input VCF using a workflow provided by the `PanGenie` project[1] We used the "high-gq" quality filter also used in the `PanGenie` study: genotype quality (GQ) $\geq$ 200. The fourth method assessed was `rowbowt`.

Prior to applying `BayesTyper`, we built a `BayesTyper`-compatible VCF file containing all relevant variants from the HGSVC haplotype panel. For `rowbowt`, we created a `rowbowt` index from the genomes in the HGSVC haplotype panel. In both cases we excluded NA12878's haplotypes from the panel prior to building the index.

When evaluating, we stratified variants by complexity: the "SNV" category includes single-nucleotide substitutions, "Indel" includes indels no more than 50bp long, and "SV" includes insertion or deletions longer than 50bp, and "All" includes all variant types. More complex structural variants like inversions and chromosomal rearrangements are ignored.

We analyzed the accuracy of `rowbowt` 's diploid genotypes in two ways. First we considered allele-by-allele precision and recall, considering the alternate (ALT) allele calls to be the positive class. Specifically, every diploid genotype called by a method is considered as a pair of individual allele calls. If a given allele call is an alternate (ALT) allele and there is at least one ALT allele present in the true diploid genotype at that site, it counts as a true positive (TP). If the given allele is a reference allele (REF) and there is at least one REF allele in the true diploid genotype, this is a true negative (TN). If the given allele is an ALT but the true genotype is homozygous REF, we count it as a false positive (FP). Finally, if the given allele is REF but the true genotype is homozygous ALT, this is a a false negative (FN).

Second, we considered precision and recall with respect to sites that were either truly heterozygous or called heterozygous. If a heterozygous call made by a method is truly heterozygous, this was counted as a true positive (TP). False positives, false negatives, and true negatives are defined accordingly.

As seen in Fig. 5, `rowbowt` 's ALT and HET precision were generally the highest of all the methods across all variant categories, though `BayesTyper` sometimes achieved higher ALT/HET precision for indels in the higher-coverage datasets and `PanGenie` had the highest HET precision for SNVs and Indels for some coverages. At the highest coverage level examined (5-fold), `PanGenie` also achieved similar ALT precision to rowbowt on SNVs and Indels. `rowbowt` dominates on precision of SV calls, and also exhibits the best recall for ALTs at higher coverage. `PanGenie` exhibits slightly higher recall for HET SVs.

Figure 6 compares the methods on their F1 measure. `rowbowt` achieved the highest F1 scores for ALT and HET SNBs. For HET SNV variants, rowbowt had the highest F1 score of 0.71, while for ALT SNV variants, the F1 was 0.95. In the case of Indel variants, rowbowt produced the highest F1 score of 0.81 for the ALT class and tied with `PanGenie` for the HET class, with an aggregate score of 0.48. Fr SVs, rowbowt had the highest F1 score of 0.55 in the ALT class and a comparable score of 0.21 in the HET class, just below `PanGenie` 's score of 0.23.

Diploid genotyping assessment on medically relevant genes

We obtained a list of medically relevant autosomal genes, collected from medical gene databases by the Genome

[1] The workflow can be found in the `pipelines/run-from-callset` subdirectory of the `PanGenie` repository.

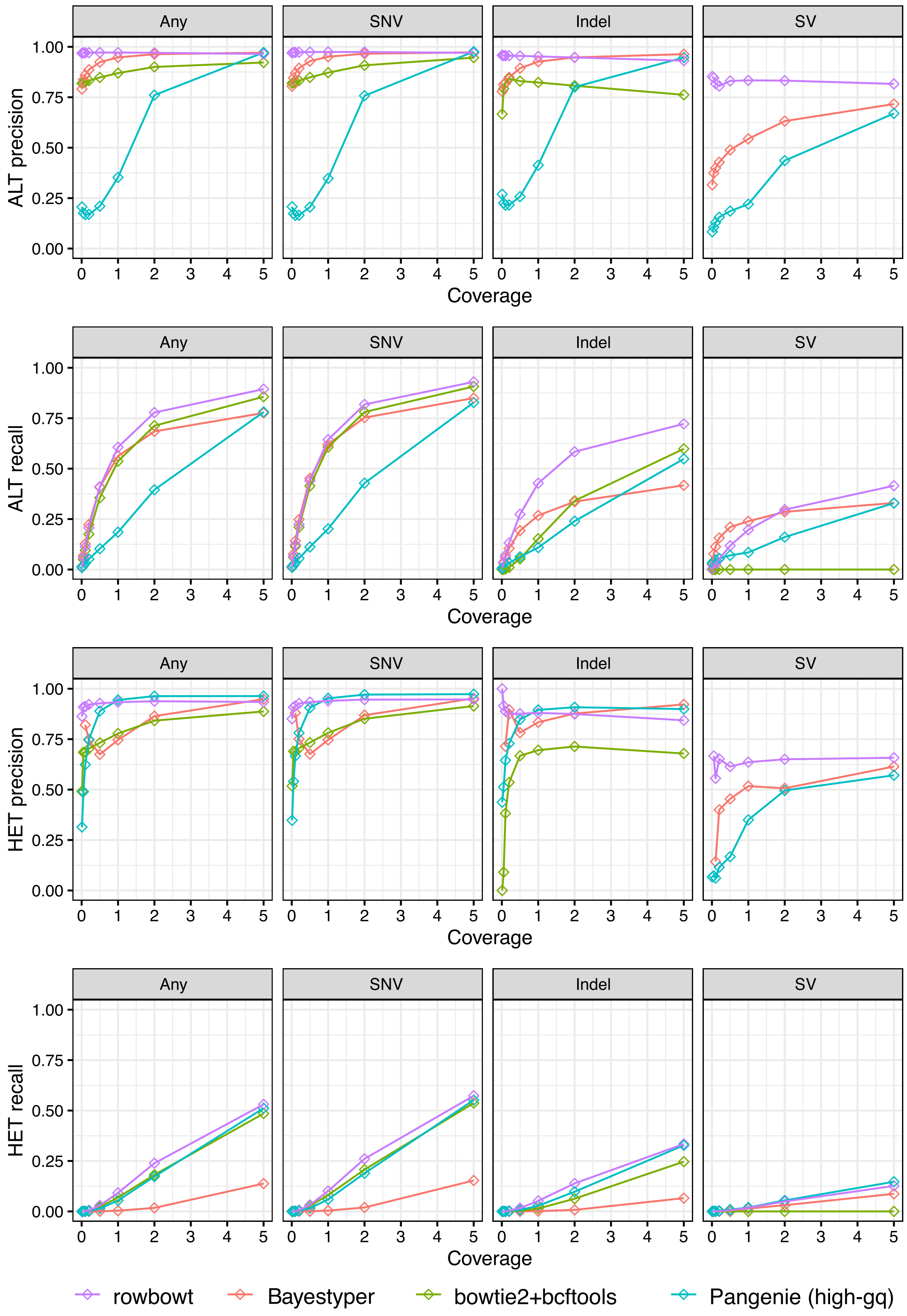

Fig. 5 Precision and recall for the four tested genotyping methods, both at the level of individual alleles (ALT precision/recall) and at the level of heterozygous variants (HET precision/recall). Note that the bowtie2+bcftools approach is generally unable to align reads across variants in the "SV" category, leading to low precision and recall

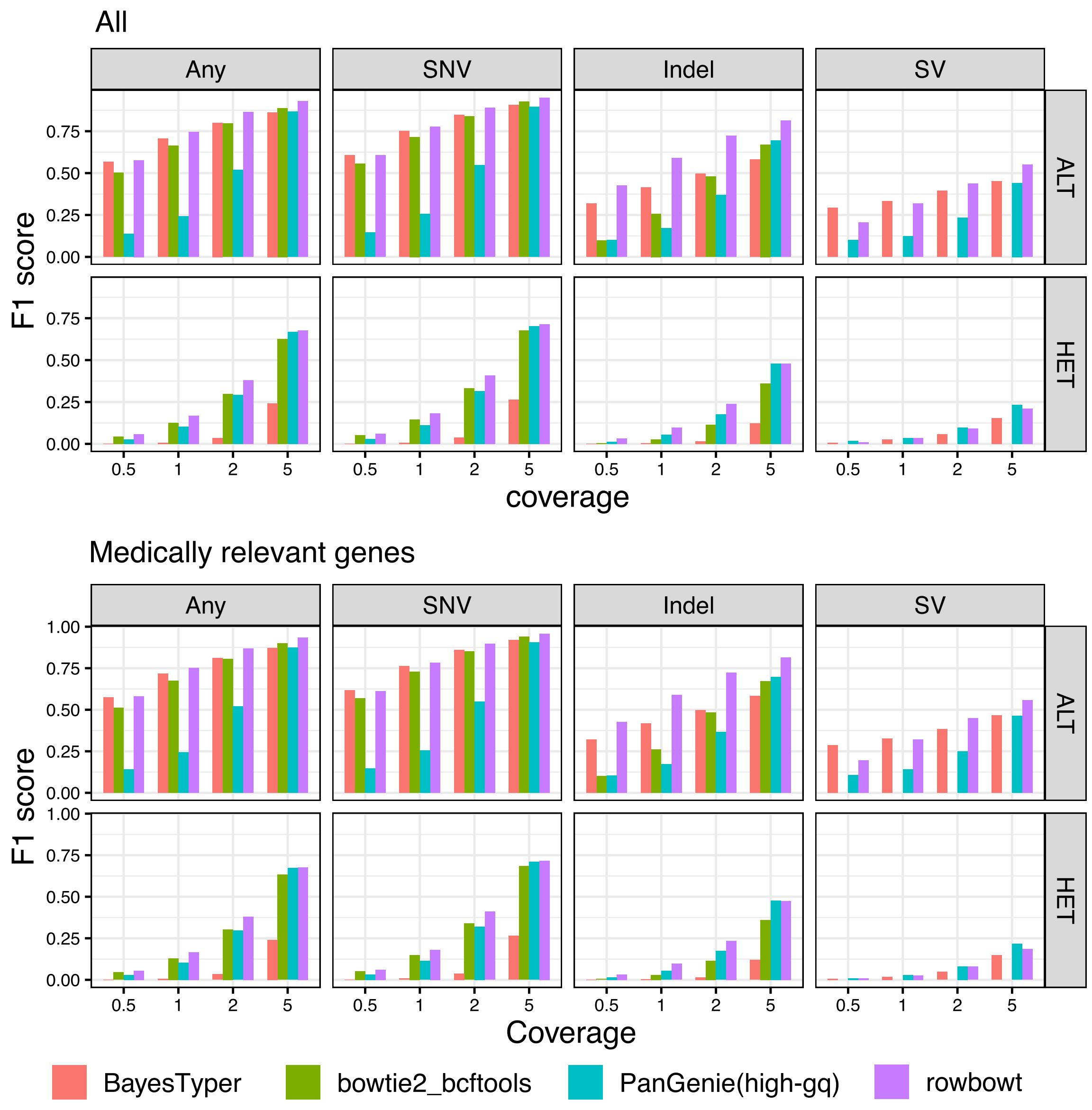

Fig. 6 F1 scores across variant types and tools. Computed genomewide (top) and over only those variants in medically relevant autosomal genes (bottom)

in a Bottle (GiaB) project [31]. Among the 5,026 genes included are the major MHC Class I genes (HLA-A, HLA-B, HLA-C), MHC Class II genes (HLA-DP, HLA-DQ, HLA-DR) and KIR genes. A complete list including coordinates can be found at the CMRG GitHub repo [32].

As seen in Fig. 7, `rowbowt` 's performance relative to the other methods is very similar for these genes compared to the full set of genes assessed in Fig. 5. As seen in Fig. 6, `rowbowt` generally outperformed other methods on F1 score for medically relevant genes. For HET SNV variants, `rowbowt` achieved the highest F1 score of 0.72, while for ALT SNV variants, the F1 score was 0.96. In the case of Indel variants, `rowbowt` was the leader with an F1 score of 0.82 for the ALT class, and tied with `PanGenie` with a score of 0.47 for the HET class. As for SVs, rowbowt had the highest F1 score of 0.56 in the ALT class, and a comparable score of 0.19 in the HET class, closely following `PanGenie` 's score of 0.22.

Computational performance

We compared the time and memory usage of each genotyping method, dividing the computations performed by each method into a few distinct categories. For each phase, we measured both the wall-clock time elapsed and

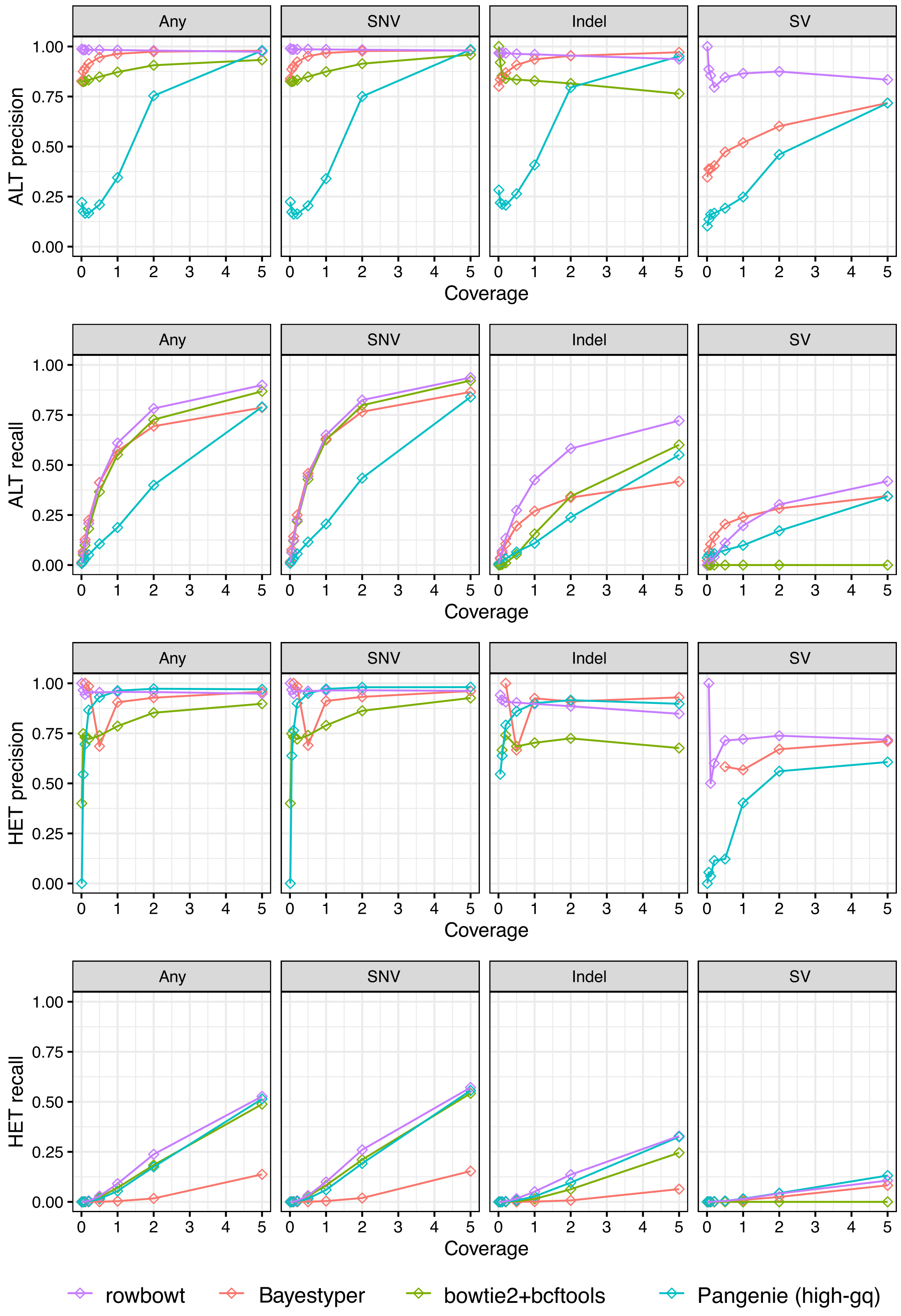

Fig. 7 Precision and recall presented as in Fig. 5 but filtered to only the medically relevant autosomal genes, collected from medical gene databases by the Genome in a Bottle (GiaB) project

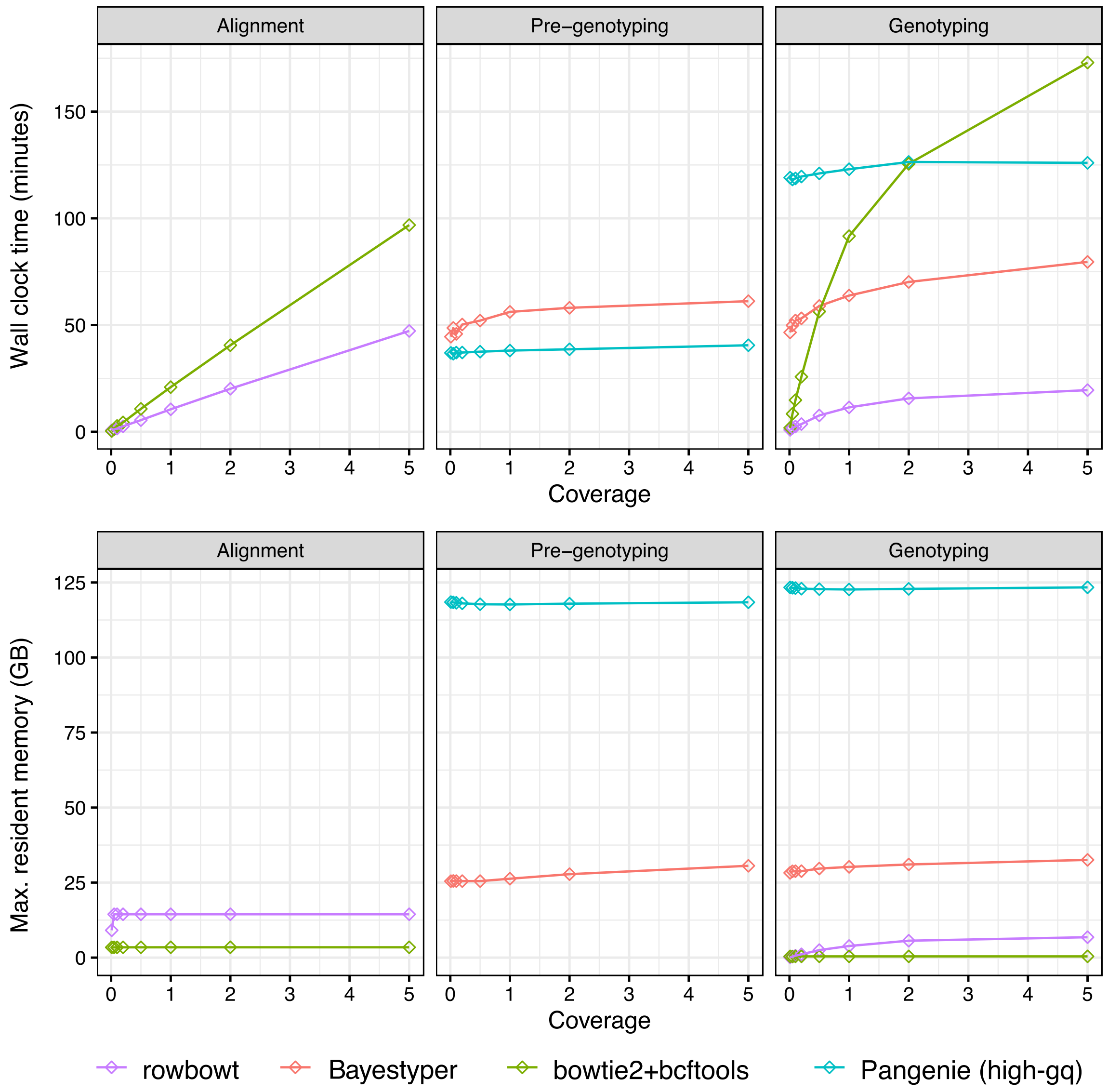

Fig. 8 Wall clock time and peak memory footprint for each phase of the genotyping workflow for four methods tested

maximum memory ("maximum resident set") used. Both were measured with the Snakemake tool's `benchmark` directive [33].

We categorized and benchmarked three distinct types of computation. For `bowtie2+bcftools`, we defined the "Alignment" step as the process of using `bowtie2` to align reads to the linear reference genome. For `rowbowt`, we defined the "Alignment" step as the process of using the `rb_markers` command to genotype the reads using the algorithm described in Methods. For the alignment-free methods `PanGenie` and `BayesTyper`, we use the term "Pre-genotyping" for the initial phase that includes *k*-mer counting and other index building procedures. In the case of `BayesTyper`, this specifically consists of (a) using the KMC3 software [34] to count *k*-mers in the input reads, (b) using the `bayestyper makeBloom` command to convert *k*-mer counts to Bloom filters for each sample, and (c) using the `bayestyper cluster` command to identify variant clusters. In the case of `PanGenie`, "Pre-genotyping" consists of: (a) reading input files, (b) *k*-mer counting, (c) path selection, (c) determining unique *k*-mers. Also for `PanGenie`, the initial input VCF file must be preprocessed into a new VCF file containing additional fields, accounting for about 1 h of computation, not included in our measurements.

16 threads were used during the Alignment phase for `bowtie2+bcftools`, `rowbowt` and `PanGenie`, while 32 threads were used for `BayesTyper`.

For `bowtie2+bcftools`, we define the Genotyping step as the process of using `bcftools call` to call variants from the BAM file output by `bowtie2`. For `rowbowt` We define the Genotyping phase as the process of running the `vc_from_markers.py` script on the output from `rb_markers`. For `BayesTyper`, we define the genotyping step as the process of running the `bayesTyper genotype` command. `PanGenie` was run by providing 16 threads. Figure 8 shows the time-taken and peak memory footprint for each method and on defined phases.

The Genotype phases for both `bowtie2+bcftools` and `rowbowt` do not support multi-threading, so a single thread was used. For the `BayesTyper` and Pangenome Genotype phases, we used 16 threads.

Figure 8 shows the time taken and peak memory footprint for each method and each category. We observed that `rowbowt` was consistently faster than the other methods in the Genotyping phase, sometimes by a large margin. We also observed that while `rowbowt` has a higher memory footprint compared to the `bowtie2+bcftools` method, it uses substantially less memory than `BayesTyper` and `PanGenie`, the other pangenome-based methods. `PanGenie` has a particularly high (>100 gigabyte) memory footprint in both the Pre-genotyping and Genotyping steps.

Discussion

We proposed a family of novel marker array structures, M, MA and MA^w that, together with a pangenome index like the r-index, allow for rapid and memory-efficient genotyping with respect to large pan-genome references. The augmented marker array is smaller and faster to query than the run-sampled suffix array — the usual way to establish where matches fall when querying a run-length compressed index — especially when we limit the set of markers to just alleles at frequency 1% or higher. We further showed that the augmented marker array can replace the sampled suffix array in simple genotyping experiments with moderate sacrifice of precision, and that a marker array based genotyping method outperforms the graph-based `BayesTyper` method.

Pan-genome indexes allow for rapid analysis of reads while reducing reference bias. The indexes used in our experiments consisted of many (up to 65) haplotypes, with none having a higher priority over the others, except in the sense that results were expressed in terms of the standard reference. Our approach preserves all linkage disequilibrium information. This is in contrast to some graph-indexing approaches, which might consider all possible combinations of nearby alleles to be "valid," even if most combinations never co-occur in nature.

While we examined only simple structural variants in the form of insertions and deletions longer than 50 bp, the genotyping method is readily extensible to more complex differences as well. Indeed, as long as we can mark the base or bases just to the left of the variant, we can mark any variant in a way that we can later genotype.

Our method will mark only a single base that is to the left of the boundary ("breakpoint") of a variant. This is true whether the variant is large (i.e. is a large insertion or deletion) or small (i.e. an SNV). We choose to mark the base to the left of the boundary rather than the right because suffixes starting from the base to the right will be unaffected by the REF and ALT alleles; therefore, matches spanning that position do not necessarily carry evidence for a particular allele. That said, an alternative approach would be to consider "suffixes" extending in either direction—either left-to-right or right-to-left—by additionally indexing the reverse of the reference sequences. If both forward and reverse versions of the index are available, our method can be made more robust by combining the evidence obtained from matches spanning both the left and right boundaries of the polymorphic variant. In the future, it will be important to measure whether the increase in index size and genotyping memory footprint can justify this refinement.

We also note that our strategy marks only a single left-flank base position per variant, even in the case of an insertion or deletion where the alleles span different numbers of bases. For instance, for an insertion where the REF allele is `A` and the ALT allele is `AGG`. If we were instead to mark both the left-flank base (`A` in this example) and every base within the insertion (the two `G`s in the ALT allele), we are vulnerable to a bias resulting from the fact that there are more opportunities to observe a match overlapping the longer allele than the shorter one. Without any correction, this artificially inflates the evidence from the longer allele. That said, it should be possible to correct for the bias, e.g. by penalizing the evidence from the longer allele in a length-weighted fashion. In the future, it will be important to investigate whether this enhanced marking strategy yields an overall improvement in genotyping accuracy.

Since this work first appeared, other groups have pursued related ideas. In particular, we note that the new MARIA index is capable list all the distinct columns of the multiple alignment overlapped by a match in the r-index [35]. Further, that study defines a quantity called r' that captures something similar to the number of distinct runs we expected to find in the MA or MA^w arrays. In the future it will be important to directly relate r' to the quantities discussed here and to compare the advantages and disadvantages of our genotyping-centric approach to the more general approach of MARIA.

The `rowbowt` method can lead to future methods that use information about genotypes to build a personalized reference genome, containing exactly the genotyped alleles. Alignment to a personalized reference have been shown previously to be the best way to reduce reference bias, even more effective than the best pangenome methods [10, 13].

Acknowledgements
We thank Massimiliano Rossi and Travis Gagie for many helpful discussions. We thank Margaret Gagie for her careful editing.Part of this research project was conducted using computational resources at the Maryland Advanced Research Computing Center (MARCC).

Author contributions
TM and BL conceived the method. TM wrote the Rowbowt software tool. TM, NGKV and BL designed and ran the experiments. TM, NGKV and BL wrote and revised the manuscript. All authors reviewed the manuscript. All authors read and approved the final manuscript.

Funding
N.S.K.V., T.M. and B.L. were supported by NIH grants R01HG011392 and R35GM139602 to BL. T.M. and B.L. were also supported by NSF DBI Grant 2029552.

Availability of data and materials
`rowbowt` is available at https://github.com/alshai/rowbowt.

Declarations

Competing interests
The authors declare that they have no competing interests.

Received: 31 March 2023 Accepted: 22 April 2023
Published online: 05 May 2023

References
1. Davies RW, Kucka M, Su D, Shi S, Flanagan M, Cunniff CM, Chan YF, Myers S. Rapid genotype imputation from sequence with reference panels. Nat Genet. 2021;53(7):1104–11.
2. Kim C, Guo H, Kong W, Chandnani R, Shuang LS, Paterson AH. Application of genotyping by sequencing technology to a variety of crop breeding programs. Plant Sci. 2016;242:14–22.
3. Auton A, Brooks LD, Durbin RM, Garrison EP, Kang HM, Korbel JO, Marchini JL, McCarthy S, McVean GA, Abecasis GR, et al. A global reference for human genetic variation. Nature. 2015;526(7571):68–74.
4. Schneider VA, Graves-Lindsay T, Howe K, Bouk N, Chen HC, Kitts PA, Murphy TD, Pruitt KD, Thibaud-Nissen F, Albracht D, et al. Evaluation of GRCh38 and de novo haploid genome assemblies demonstrates the enduring quality of the reference assembly. Genome Res. 2017;27(5):849–64.
5. Günther T, Nettelblad C. The presence and impact of reference bias on population genomic studies of prehistoric human populations. PLoS Genet. 2019;15(7):1008302.
6. Brandt DY, Aguiar VR, Bitarello BD, Nunes K, Goudet J, Meyer D. Mapping bias overestimates reference allele frequencies at the HLA genes in the 1000 genomes project phase I data. G3 (Bethesda). 2015;5(5):931–41.
7. Sherman RM, Forman J, Antonescu V, Puiu D, Daya M, Rafaels N, Boorgula MP, Chavan S, Vergara C, Ortega VE, et al. Assembly of a pan-genome from deep sequencing of 910 humans of African descent. Nat Genet. 2019;51(1):30–5.
8. Denti L, Previtali M, Bernardini G, Schönhuth A, Bonizzoni P. MALVA: genotyping by mapping-free ALlele detection of known VAriants. iScience. 2019;18:20–7.
9. Shajii A, Yorukoglu D, William Yu Y, Berger B. Fast genotyping of known SNPs through approximate k-mer matching. Bioinformatics. 2016;32(17):538–44.
10. Pritt J, Chen NC, Langmead B. FORGe: prioritizing variants for graph genomes. Genome Biol. 2018;19(1):220.
11. Chen S, Krusche P, Dolzhenko E, Sherman RM, Petrovski R, Schlesinger F, Kirsche M, Bentley DR, Schatz MC, Sedlazeck FJ, Eberle MA. Paragraph: a graph-based structural variant genotyper for short-read sequence data. Genome Biol. 2019;20(1):291.
12. Garrison E, Sirén J, Novak AM, Hickey G, Eizenga JM, Dawson ET, Jones W, Garg S, Markello C, Lin MF, Paten B, Durbin R. Variation graph toolkit improves read mapping by representing genetic variation in the reference. Nat Biotechnol. 2018;36(9):875–9.
13. Chen NC, Solomon B, Mun T, Iyer S, Langmead B. Reference flow: reducing reference bias using multiple population genomes. Genome Biol. 2021;22(1):8.
14. n J, Monlong J, Chang X, Novak AM, Eizenga JM, Markello C, Sibbesen JA, Hickey G, Chang PC, Carroll A, Gupta N, Gabriel S, Blackwell TW, Ratan A, Taylor KD, Rich SS, Rotter JI, Haussler D, Garrison E, Paten B. Pangenomics enables genotyping of known structural variants in 5202 diverse genomes. Science. 2021;374(6574):8871.
15. Sibbesen JA, Maretty L, Krogh A. Accurate genotyping across variant classes and lengths using variant graphs. Nat Genet. 2018;50(7):1054–9.
16. Ebler J, Ebert P, Clarke WE, Rausch T, Audano PA, Houwaart T, Mao Y, Korbel JO, Eichler EE, Zody MC, et al. Pangenome-based genome inference allows efficient and accurate genotyping across a wide spectrum of variant classes. Nat Genet. 2022;54(4):518–25.
17. Gagie T, Navarro G, Prezza N. Optimal-Time Text Indexing in BWT-runs Bounded Space. In: Proceedings of the 29th Annual Symposium on Discrete Algorithms (SODA), pp. 1459–1477; 2018.
18. Kuhnle A, Mun T, Boucher C, Gagie T, Langmead B, Manzini G. Efficient construction of a complete index for pan-genomics read alignment. J Comput Biol. 2020;27(4):500–13.
19. Ahmed O, Rossi M, Kovaka S, Schatz MC, Gagie T, Boucher C, Langmead B. Pan-genomic matching statistics for targeted nanopore sequencing. iScience. 2021;24(6): 102696.
20. Burrows M, Wheeler DJ. A block sorting lossless data compression algorithm. Technical Report 124, Digital Equipment Corporation 1994.
21. Ferragina P, Manzini G. Opportunistic data structures with applications. In: Proceedings of the 41st Annual Symposium on Foundations of Computer Science (FOCS), pp. 390–398; 2000.
22. Chaisson MJP, Sanders AD, Zhao X, Malhotra A, Porubsky D, Rausch T, Gardner EJ, Rodriguez OL, Guo L, Collins RL, et al. Multi-platform discovery of haplotype-resolved structural variation in human genomes. Nat Commun. 2019;10(1):1784.
23. Ebert P, Audano PA, Zhu Q, Rodriguez-Martin B, Porubsky D, Bonder MJ, Sulovari A, Ebler J, Zhou W, Serra Mari R, et al. Haplotype-resolved diverse human genomes and integrated analysis of structural variation. Science. 2021;372:6537.
24. Rossi M, Oliva M, Langmead B, Gagie T, Boucher C. MONI: a pangenomic index for finding maximal exact matches. J Comput Biol. 2022;29(2):169–87.
25. Danecek P, Auton A, Abecasis G, Albers CA, Banks E, DePristo MA, Handsaker RE, Lunter G, Marth GT, Sherry ST, et al. The variant call format and VCFtools. Bioinformatics. 2011;27(15):2156–8.
26. Li H. A statistical framework for SNP calling, mutation discovery, association mapping and population genetical parameter estimation from sequencing data. Bioinformatics. 2011;27(21):2987–93.
27. Gog S, Beller T, Moffat A, Petri M. From theory to practice: Plug and play with succinct data structures. In: 13th International Symposium on Experimental Algorithms, (SEA 2014), pp. 326–337; 2014.
28. Belazzougui D, Cunial F, Gagie T, Prezza N, Raffinot M. Flexible indexing of repetitive collections. In: Kari J, Manea F, Petre I., editors. Unveiling dynamics and complexity. vol. 10307, pp. 162–174. Springer, Cham; 2017. Series Title: Lecture Notes in Computer Science.
29. Reinert K, Dadi TH, Ehrhardt M, Hauswedell H, Mehringer S, Rahn R, Kim J, Pockrandt C, Winkler J, Siragusa E, Urgese G, Weese D. The SeqAn C++

template library for efficient sequence analysis: A resource for programmers. J Biotechnol. 2017;261:157–68.
30. Langmead B, Salzberg SL. Fast gapped-read alignment with Bowtie 2. Nat Methods. 2012;9(4):357–9.
31. Wagner J, Olson ND, Harris L, McDaniel J, Cheng H, Fungtammasan A, Hwang Y-C, Gupta R, Wenger AM, Rowell WJ, et al. Towards a comprehensive variation benchmark for challenging medically-relevant autosomal genes. 2021.
32. NIST: Medically Relevant Genes. [Online]. Available from: https://github.com/usnistgov/cmrg-benchmarkset-manuscript/tree/master/data/gene_coords/unsorted/GRCh38_mrg_full_gene.bed. Accessed 19 Mar 2023.
33. Mölder F, Jablonski KP, Letcher B, Hall MB, Tomkins-Tinch CH, Sochat V, Forster J, Lee S, Twardziok SO, Kanitz A, Wilm A, Holtgrewe M, Rahmann S, Nahnsen S, Köster J. Sustainable data analysis with Snakemake. F1000 Res. 2021;10:33.
34. Kokot M, Dlugosz M, Deorowicz S. KMC 3: counting and manipulating k-mer statistics. Bioinformatics. 2017;33(17):2759–61.
35. Goga A, Baláž A, Petescia A, Gagie T. MARIA: multiple-alignment r-index with aggregation. 2022. arXiv 2209.09218.

Publisher's Note